processes

MDPI

Article

Wastewater Treatment Using Shear Enhanced Flotation Separation Technology: A Pilot Plant Study for Winery Wastewater Processing

David Vlotman *, David Key, Bradley Cerff and Bernard Jan Bladergroen

Department of Chemistry, South African Institute for Advanced Materials Chemistry (SAIAMC), Faculty of Natural Sciences, University of the Western Cape, Cape Town 7535, South Africa; dkey@uwc.ac.za (D.K.); bcerff@uwc.ac.za (B.C.); bbladergroen@uwc.ac.za (B.J.B.)

* Correspondence: 4056787@myuwc.ac.za; Tel.: +27-21-959-9309

Abstract: The agricultural sector is one that requires and consumes enormous amounts of fresh water globally. Commercial wine production in particular uses large volumes of fresh water and, through various processes, generates significant quantities of wastewater. The wastewater produced by wineries typically exhibits elevated levels of chemical oxygen demand (COD), total suspended solids (TSS), an acidic pH, and varying salinity and nutrient contents. The overall characteristics of winery wastewater indicate that it is a potential environmental hazard if not processed and disposed of appropriately. Due to significant variations in wastewater contaminant levels among wineries, the implementation of a universally applicable, environmentally friendly, and sustainable waste management system seems practically unattainable. This study investigated the design, fabrication, and modification of a shear enhanced flotation separation (SEFS) pilot plant to be used as a primary treatment stage during winery wastewater processing. This technology combines the synergistic advantages of hydrodynamic shear, coagulation, flocculation, and dissolved air flotation. To date, there have been only limited publications on the feasibility and application of hydrodynamic shear and its potential to assist with coagulation/flocculation and flotation efficiencies specifically for winery wastewater treatment. The results obtained indicate that the SEFS pilot plant may well be able to process winery wastewater to a quality level where reuse of the water for irrigation of crops may be considered.

Keywords: agriculture; coagulation; COD; colloids; dissolved air flotation; flocculation; hydrodynamic shear; suspended solids; winery wastewater; zeta potential

Citation: Vlotman, D.; Key, D.; Cerff, B.; Bladergroen, B.J. Wastewater Treatment Using Shear Enhanced Flotation Separation Technology: A Pilot Plant Study for Winery Wastewater Processing. *Processes* **2024**, *12*, 3. https://doi.org/10.3390/pr12010003

Academic Editors: Maria Angélica Simoes Dornellas De Barros and Thiago Peixoto De Araújo

Received: 16 November 2023
Revised: 13 December 2023
Accepted: 14 December 2023
Published: 19 December 2023

1. Introduction

The wine industry is known to consume large volumes of fresh water, subsequently generating substantial amounts of wastewater and solid waste during production processes [1]. This waste stream is often characterized by high concentrations of both organic and inorganic contaminants, which, if left untreated, may have negative impacts on the environment [2].

Wine waste consists of a matrix of solid and liquid components. The solid components in wine wastes are generated during processes such as destemming, pressing, filtration, and settling. The solid waste is composed of skins, stems, excess grape pulp, seeds, stalks, and yeast cells that are generated during the process of fermentation [3]. In relation to percentage composition, it consists of 7.5% grape stems, up to 45% grape pomace, and approximately 6% grape seeds [4]. The liquid component, i.e., winery wastewater, on the other hand, is generated during the cleaning of barrels and tanks, washing of transfer lines and floors, wine extraction, as well as numerous other operations in filtration units and water drains [5].

For every ton of grapes processed, wineries typically produce 3–5 cubic meters of wastewater [6]. To contextualize this, the South African wine sector processed 1.2 million tons of grapes in total during the 2022 harvest season [7]. As a result, the total volume of wastewater generated in this specific vintage season is estimated at approximately between 3.6 and 6 million cubic meters [8]. Comparatively, the Australian wine grape crush for the 2022 harvest season was 1.7 million metric tons, implying that 5–10 million liters of wastewater was generated [9]. An estimated 10.5 to 17.5 million cubic meters of wastewater was produced during the vintage season in 2022 as a result of the joint processing of 3.6 million tons of grapes by the California wine production business in the United States [10].

The generation of these extensive quantities of wastewater is a cause for concern considering the world's ongoing population growth and scarce water resources, which contribute to the challenge of limited access to clean fresh water [11,12]. The volume of winery wastewater produced poses additional sustainability-related difficulties in terms of environmentally sustainable discharge and reuse. This is made worse by the variable consistency and quality of wastewater from wineries, which fluctuates seasonally and typically contains chemical compounds that are harmful to the environment. As such, ensuring that appropriate treatment and disposal are consistently carried out becomes an essential objective for wineries [13].

Winery wastewaters are notorious for their acidic pH, which is linked to the presence of various organic acids [14,15]. The electrical conductivity (EC) of winery wastewater may reach values up to 6.15 mS/cm [16]. Nutrients in winery wastewater have caused high reported levels of total nitrogen (TN) and total phosphorous (TP) at 640 mg/L and 657 mg/L, respectively [17,18]. Chemical oxygen demand (COD) values routinely seen in winery wastewater generally fall within the range of 300 mg/L to the possibility of reaching values of up to 300,000 mg/L [19–21].

There are serious and diverse environmental consequences linked to the unsafe discharge of wastewater from wineries into the environment [15]. These include the release of foul odors mainly due to the high organic content of the wastewater, the degradation of soil quality, damage to vegetation as a result of wastewater disposal techniques, and overall pollution of water bodies [22]. Based on these adverse environmental effects, wineries are requested to treat their wastewater to regulated standards before being discharged into the environment.

Coagulation and flocculation have, to date, been the staple processes during water and wastewater treatment [23–25]. Generally, colloidal particles present in wastewater are negatively charged. The presence of these negative charges produces repulsion forces within the medium, hence decreasing the tendency of particles to aggregate, form floccules (flocs), and enhance sedimentation and flotation techniques. There have been extensive reports and literature studies related to conventional and emerging winery wastewater treatment options [20,26–29]. However, many of these technologies are more applicable to treat wastewater from medium- to large-scale wineries rather than those from the many small wineries. A relatively new and emerging treatment option involves the use of hydrodynamic shear mixing with flotation [30].

Hydrodynamic shear mixing has been previously used during emulsion processing as well as for the possessing of tight stable emulsions in petroleum wastewater treatment [31,32]. The basic principle of this technology involves the intentional destabilization of colloidal suspensions. This destabilization is achieved by subjecting the suspension to shear flow through mechanical agitation. The primary objective of this process is to facilitate the aggregation of micron-sized solid particles, resulting in the formation of larger flocs, which are more effectively separated from the liquid phase [33].

The aggregation of colloidal particles is facilitated by shear flow through two primary mechanisms. In the case of kinetically stabilized colloidal suspensions exhibiting a sufficiently high energy barrier that prevents aggregation, it is possible for the convective energy (process of thermal energy exchange in fluids via the motion of matter within

them) transmitted by the fluid to facilitate the particles to overcome the repulsive barrier and undergo aggregation. In the second situation, when dealing with totally destabilized suspensions, the rate of collisions is solely determined by the strength of the flow field. This leads to a significant acceleration of the aggregation kinetics in comparison to a purely diffusive mechanism [34].

High shear mixers (HSMs) are considered to be an innovative and appealing form of process intensification equipment [35]. These mixers show great potential with regard to enhancing the liquid–liquid extraction process inside solid–liquid–liquid systems. However, there is a scarcity of literature reporting on this particular aspect.

High shear mixers, much like flotation devices, have mostly been used in emulsion and mineral processing [33,36–38]. However, their potential to serve as an alternative treatment method for winery wastewater is yet to be proven. The potential of this technology to alter particle size as well as surface charges of colloidal particles needs to be explored in further detail, specifically in a practical sense.

This study focused on the key parameters of turbidity, total suspended solids (TSS), and particulate chemical oxygen demand (COD) in relation to the efficiency of winery wastewater treatment utilizing a hybrid shear enhanced flotation separation (SEFS) pilot plant. Due to the complexity of the treatment system (a nonsymmetrical system), which consists of a multiphase medium, the shear rate/speed in the rotor stator mixer configuration is an intricate parameter to quantify. As such, the terms shear rate/speed used throughout this paper have been simplified and quantified using revolutions per minute (rpm).

2. Materials and Methods

2.1. Untreated Winery Wastewater Collection

The winery wastewater used in this study was collected directly from a winery situated in the West Coast region of South Africa during the vintage period in April 2023. This untreated wastewater was used as feed water for batch experiments. The inherent wastewater treatment process at the winery involves the gravitational transfer of wastewater from the cellar, passing through a 2 mm screen grid. This grid separates a large portion of the solid substances, which is composed of a variety of substances including skins, seeds, stems, residual pulp, fragments of stalks, and yeast cells. The initial untreated wastewater for the pilot plant experiments was obtained from the waste stream, below the 2 mm screen grid, and transferred into a sequence of intermediate bulk containers (IBCs) using a Pedrollo RX2/20 submersible pump. The IBCs were relocated to the pilot plant facility located at the University of the Western Cape, Bellville, South Africa.

2.2. Alkalization Study

The experimental investigations for alkalization studies were carried out in 6 × 1000 L IBCs under standard ambient conditions of pressure and temperature. A lime slurry solution was prepared by mixing 10 kg of hydrated lime ($(CaOH)_2$) sourced from Cape Lime (Pty) Ltd. in Vredendal, South Africa, with 100 L of tap water. The pH of the untreated effluent, initially at pH 4, was adjusted to a pH of 9 by adding 9% w/w of lime slurry to an initial starting volume of 800 L winery wastewater.

2.3. Pilot Plant P&ID

A pilot plant system was designed utilizing a conventional DAF treatment unit with the integration of a hydrodynamic shear mixer to treat winery wastewater at a rate of 5 L/min. The piping and instrumentation diagram (P&ID) of the pilot plant treatment system is illustrated in Figure 1.

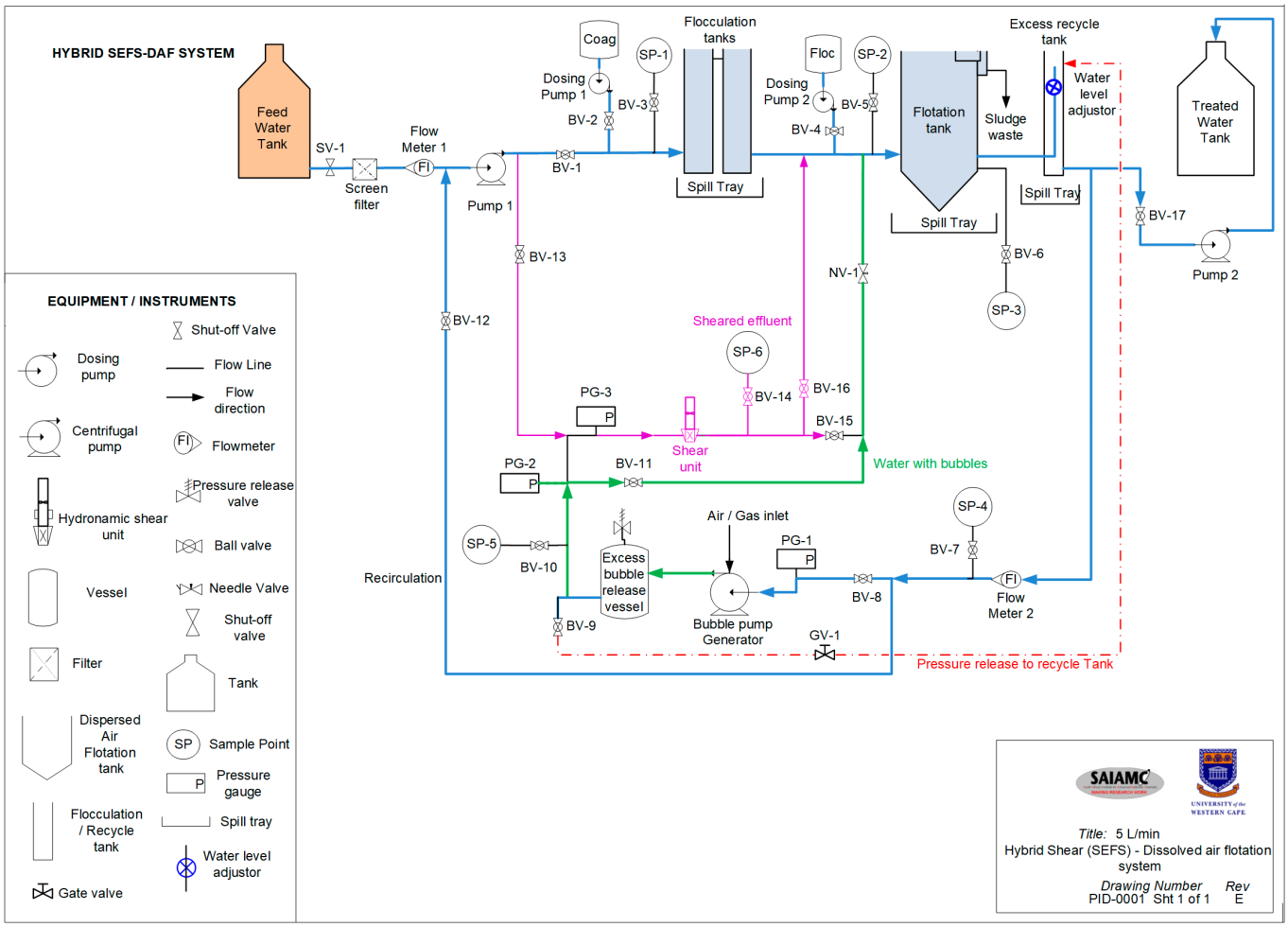

Figure 1. P&ID of the hybrid SEFS/DAF treatment system.

The pilot plant system consisted of intermediate bulk containers (IBC) flocculation tanks, a stainless-steel flotation tank, a recycle tank, an excess bubble release vessel, a microbubble generation pump, chemical dosing vessels, chemical dosing pumps, a needle valve (NV), gate valve (GV), shut off valve (SV), water level adjustor, flow meters (Fl), and ball valves (BV). The objective of the system is to study the extent to which organic and inorganic pollutants in winery wastewater can be removed utilizing hydrodynamic shear, coagulation, flocculation, and dissolved air flotation.

During experimental tests, the preconditioned winery wastewater (pH adjusted with lime slurry) was introduced and circulated through the unit until the pressure at PG-2 was stabilized at 2.5 bar. At this point, only BV-1 and BV-12 were open. After reaching this steady state, various processes and parameters were investigated, which included conventional dissolved air flotation treatment,) where coagulation (BV-2), flocculation (BV-4), and microbubbles (BV-8 inlet, and BV-11 outlet (as indicated by the green line)) and needle valve (NV-1) is opened. A hydrodynamic shear mixing unit was added (pink line) where the wastewater can be exposed to excessive mechanical agitation by way of shear. This is achieved by opening BV-13 and BV-16. The system was designed so that each individual subsystem could be tested as well as to test the synergistic effects of these subsystems.

The sampling points (SP) for each stage of treatment is as follows:

- Coagulation (BV-3 and SP-1);
- Flocculation (BV-5 and SP-2);
- DAF-treated wastewater (BV-6 and SP-3);

- Recycled water (BV-7 and SP-4);
- Microbubble infused water (BV-10 and SP-5);
- Sheared wastewater (BV-14 and SP-6).

2.4. Coagulation and Flocculation

In this investigation, the selection of treatment chemicals was based on the efficacy of aluminum-based polymeric coagulants and polyacrylamide flocculants in treating diverse types of wastewater [25,39–43]. The coagulant used during this study was a 1% (*w*/*w*) ACHD65, a composite of polydiallyldimethylammonium chloride (polydadmac) and aluminum chlorohydrate (ACH), having a specific gravity of 1.2. Polyacrylamide (PAM) granules served as the flocculant and were prepared as a 1% (*w*/*w*) solution using ultrapure deionized water obtained from a Milli-Q system manufactured by Millipore Co. in Billerica, MA, USA. The coagulant and flocculant chemicals were procured from Aqua Aero Vitae (Pty) Ltd., a company based in Cape Town, South Africa. This part of the study aimed to examine the impact of varying coagulant dosages on preconditioned wastewater samples with a pH level of 9. Zeta potential analysis was conducted to assess the ideal dosage of the coagulant based on the absolute surface charge reduction (i.e., destabilization) of the particles in the wastewater.

Coagulation and Flocculation Dosages

A typical jar test was conducted for chemical experiments. This method facilitates adjusting of pH as well as variations in coagulant and flocculant dosage to predict the effectiveness of a treatment plant operating on a larger scale. The experimental conditions related to coagulant and flocculant dosage have been described in a laboratory-scale study to treat winery wastewater [44]. Briefly, 4 × 400 mL samples of preconditioned wastewater were subjected to various dosages of coagulant and flocculant in order to determine optimum dosages to be used in the pilot plant study. The jar tests were conducted in a FC4S VELP Scientific jar test unit (South Africa) using 76 × 25 mm flat paddle impellers at room temperature (23 ± 1.0 °C), as shown in Figure 2.

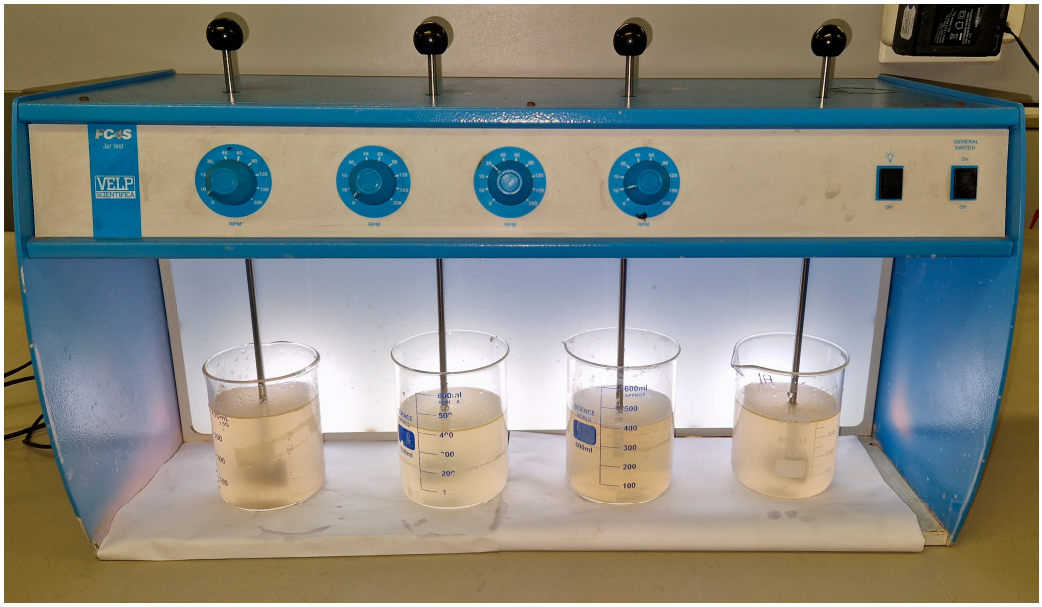

Figure 2. VELP Scientific jar test apparatus used during jar tests.

In a typical coagulation experiment in the pilot plant, aliquots of coagulant were added directly to the preconditioned wastewater via BV-2. Coagulation experiments occurred with and without the addition of shear (BV-14, BV-15, and BV-16 closed) and microbubbles (BV-8, BV-11, and NV-1 closed). Samples were extracted from the sample points SP-1 and

SP-4 and taken immediately for zeta potential analysis. Flocculation experiments followed coagulation where a predetermined concentration of PAM (aided by the jar tests) was injected into BV-4 in order to facilitate the aggregation of coagulated particles. Samples for flocculation experiments were extracted 15 min after recycling through SP-2 and SP-4 and analyzed for turbidity and total suspended solids.

2.5. High Shear Mixing

The shear unit was fabricated using steel sheets that were assembled to provide a sturdy external framework, accompanied by an internally rotating watertight unit, as illustrated in Figure 3. The multilayered steel structure facilitates the creation of an extended shear gap of 1.3 mm between the rotor and stator, allowing for the passage of wastewater through an entry and exit point. Rotational speed (in rpm) of the mixer was quantified using a high-precision tachometer, DT2236E (Addendorff, Cape Town, South Africa). The shear mixer presented in Figure 3 is currently part of a patent that has been filed and the exact details of the mixer will be presented in future work by the authors [45].

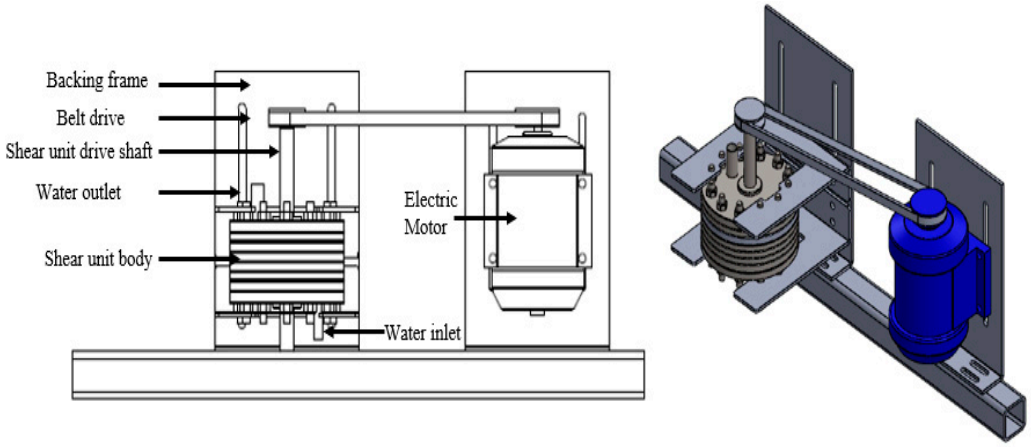

Figure 3. Driving belt connected to the shear unit assembly via an electric motor.

2.6. Analytical Methods

2.6.1. pH and Electrical Conductivity

The pH and electrical conductivity (EC) measurements were performed with a portable multimeter (Hach, HQ40d, Randburg, South Africa) equipped with a conductivity probe. The determination of total dissolved solids (TDS) was accomplished by multiplying the electrical conductivity (EC) values with a conversion factor. The average conversion factor from EC measured in millisiemens per meter (mS/m) at a temperature of 25 °C to TDS measured in milligrams per liter (mg/L) has been documented as 6.5 [46].

2.6.2. Turbidity

The turbidity of the samples was quantified using a Hach TL2350 turbidimeter equipped with a tungsten filament lamp, which was obtained from Agua Africa CC (Hach, South Africa). Turbidity measurements were conducted using the nephelometric method. The turbidity meter allowed for measurement values ranging from 0 to 10,000 nephelometric turbidity units (NTU).

2.6.3. Chemical Oxygen Demand

The term "chemical oxygen demand" refers to the quantification of the amount of oxygen required to oxidize the organic matter present in a sample using strong chemical oxidants such as potassium permanganate or potassium dichromate [47]. This test is widely employed as an indicator of wastewater quality.

The COD of the samples was measured using a Thermo Fisher Scientific (Waltham, MA, USA) Orion Aquafast 3140 colorimeter in combination with an Orion COD165 Ther-

moreactor. The reagent vials used in this study were the Aquafast COD HR (High Range), 0–15,000 ppm Thermo Fisher Scientific (Waltham, MA, USA).

2.6.4. Zeta Potential

The measurement of zeta potential pertains to the surface charge of particles that are suspended in a medium. Its relevance in the context of wastewater applications lies in its capacity to quantify charge neutralization. The zeta potential is a quantification of the difference in electrical potential between the surface of a particle and the surrounding solution.

The examination of zeta potential (ZP) was performed using a Malvern Zetasizer NanoZS (Malvern Instruments Ltd., Worcestershire, UK) series, which employs the electrophoretic light scattering measurement technique [48]. The investigation focused on analyzing the zeta potential measurements with respect to changes in coagulant dosage and application of various shear speeds. The laser employed in the Malvern Zetasizer Nano instrument was a 4 mW helium–neon (He-Ne) laser with a wavelength of 633 nm [48]. A dip cell (Malvern Instruments Ltd., Worcestershire, UK) was utilized for the measurement of zeta potential. The dip cell was equipped with palladium electrodes (ZEN1002).

2.7. Total Suspended Solids

Total suspended solids (TSS) were determined according to ASTM D5907–18 [49].

2.8. Bubble Size Analysis

An RS PRO USB Digital Microscope was used to capture images of bubbles produced during the treatment process. This microscope has a magnification ratio of 20× to 230× (optical zoom) and a capture resolution of 1920 × 1080. The examination of bubble size was performed using the ImageJ software package designed for Windows operating systems. ImageJ is opensource, Java-based image processing software; version 1.54d, (https://imagej.net/ij), that is similar to NIH Image, a component of the National Institute of Health in the United States of America [50].

2.9. Particle Size Analysis

The particle size of the wastewater was analyzed using a Microtrac S3500 Laser Diffraction Analyzer. Microtrac laser diffraction technology uses scattered light from multiple laser beams projected through a stream of particles. The amount and direction of light scattered by the particles are measured using an optical detector array and then analyzed using Microtrac Software (Microtrac FLEX 12.1.0.0).

3. Results

3.1. Winery Wastewater Composition

The average untreated winery wastewater composition during the 2023 harvest is illustrated in Table 1. The data displayed are consistent with the characteristics of the untreated winery wastewater reported in the literature [51–54].

Table 1. Average untreated winery wastewater characteristics.

Sampling Date	pH	Turbidity	EC	TSS	COD
	(25 °C)	(NTU)	(mS/m)	(mg/L)	(mg/L)
3–7 April 2023	3.2	849	430	2620	11,140

The pH, EC, TSS, and COD are especially important when considering using the wastewater for irrigation purposes as outlined by the general water authorizations in South Africa [55]. The legislated limits state that, in order to irrigate with wastewater of up to 50 m^3/day, the pH, EC, TSS, and COD must fall within the limits of 6–9. <200 mS/m, <25 mg/L and <5000 mg/L, respectively. Based on the wastewater characteristics presented

in Table 1, it is evident that intervention is required in order to address the environmental impacts should this wastewater be disposed of in its untreated state.

3.2. Shear Speed

The effect of shear speed was investigated based on the zeta potential of the colloids, as illustrated in Figure 4. The adopted rotation speed of the shear mixer in this study was determined as 3250 rpm. This speed was based on optimal changes in surface charge of the particles determined using zeta potential analysis. Increasing the rotational speed of the shear mixer above 3250 rpm had no significant impact on further destabilizing the particles in solution.

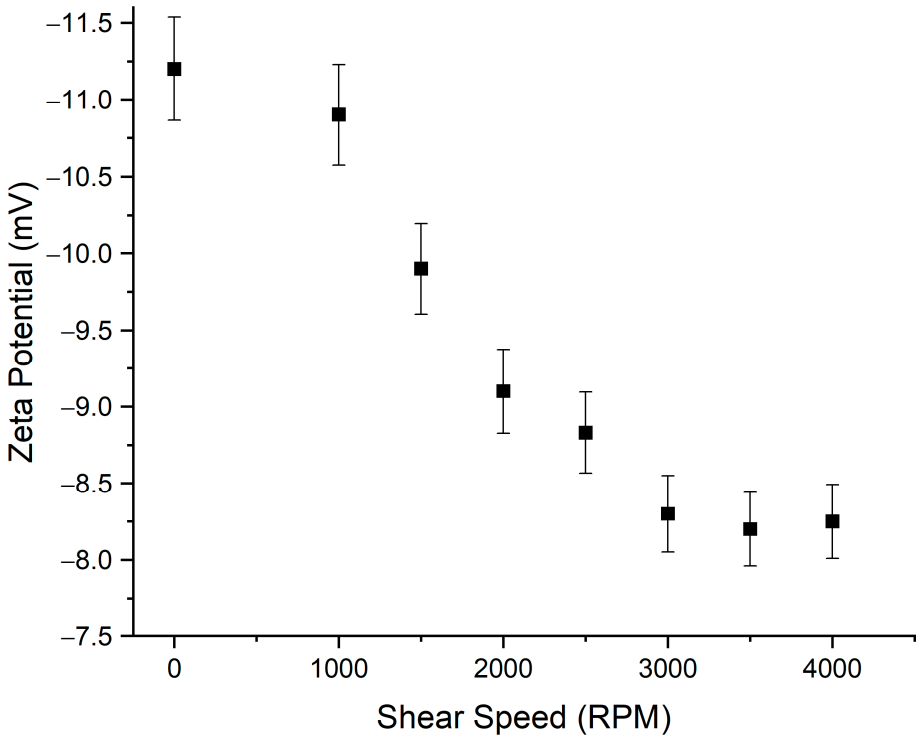

Figure 4. Shear speed as a function of zeta potential.

3.3. Particle Size Distribution

The particle size of untreated and treated wastewater is shown in Table 2.

Table 2. Particle size (in μm) of winery wastewater.

Sample	d10 [1]	d50 [2]	d90 [3]
Untreated	2.205	7.99	34.45
DAF	5.49	15.36	40.79
SEFS	10.49	23.65	56.19

[1]. Size of particle in microns below which 10% of the sample lies. [2]. Size of particle in microns at which 50% of the sample is smaller and 50% is larger. [3]. Size of particle in microns below which 90% of the sample lies.

The particle size distribution of untreated, DAF-, and SEFS-treated wastewater is shown in Figure 5.

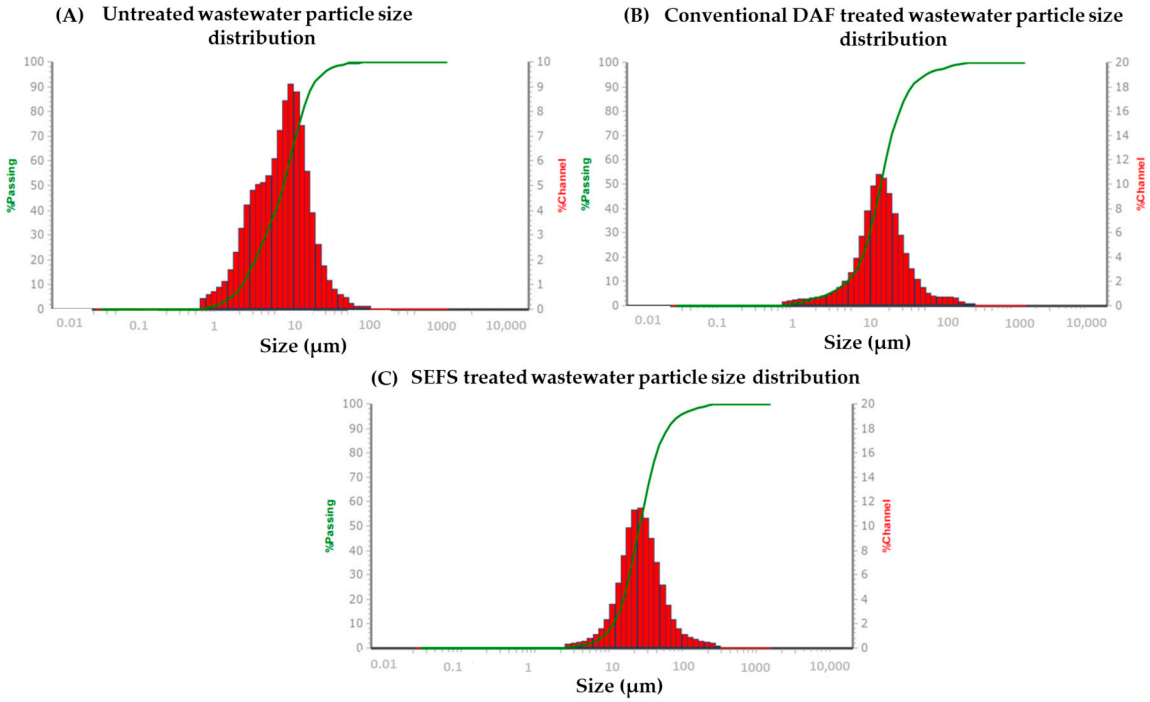

Figure 5. Particle size distribution of (**A**) untreated, (**B**) conventional DAF-, and (**C**) SEFS-treated winery wastewater.

The particle size distribution (PSD) from Table 2 and Figure 5 displays a general increase in PSD from untreated wastewater to conventional DAF- and SEFS-treated wastewater. The particles contained in the untreated wastewater had a mean diameter (D50) of 7.99 µm. When the wastewater was subjected to DAF treatment (in the absence of hydrodynamic shear), the average D50 particle size was 15.36 µm.

The increase in particle size may be attributed to the effect of coagulation and flocculation processes, which induces the process of particle destabilization by charge neutralization followed by bringing together the destabilized particles form a larger agglomerate that is removed during flotation [25]. The SEFS-treated wastewater, on the other hand, displayed average D50 particle size values of 23.65 µm. This significant growth in particle size is attributed to the hydrodynamic shear mixing, which induces agglomeration and subsequently causes colloidal destabilization of the particles in solution [56]. It is reported in the literature that particles agglomerate faster when exposed to shear due to an increase in particle collisions [57]. With reference to the PSD, it is evident that both DAF as well as SEFS results in the aggregation of colloidal particles, demonstrating the formation of larger particles, subsequently enhancing the separation process.

3.4. Zeta Potential Analysis

In aqueous systems, it is common for solid particles to possess various surface charges. These charges are often counterbalanced by oppositely charged counterions present in the solution. The resulting structure is commonly referred to as the electric double layer (EDL) [58]. Electric double layers have a significant impact on the physical and chemical properties of heterogeneous systems. The EDL model is a key concept for understanding how electrostatic force works and how it affects the stability of colloids. Therefore, it is important to have methods that can accurately determine the charge state of solid surfaces in relation to key solution factors, such as pH, ionic strength, or solute composition. The zeta potential is often used to deduce and represent significant physical and chemical characteristics of interfacial systems, including aqueous particle suspensions, due to its association with surfaces charges. This extends to the factors influencing colloidal stability and aggregation [59].

Figure 6 illustrates the correlation between the zeta potential and each respective treatment phase.

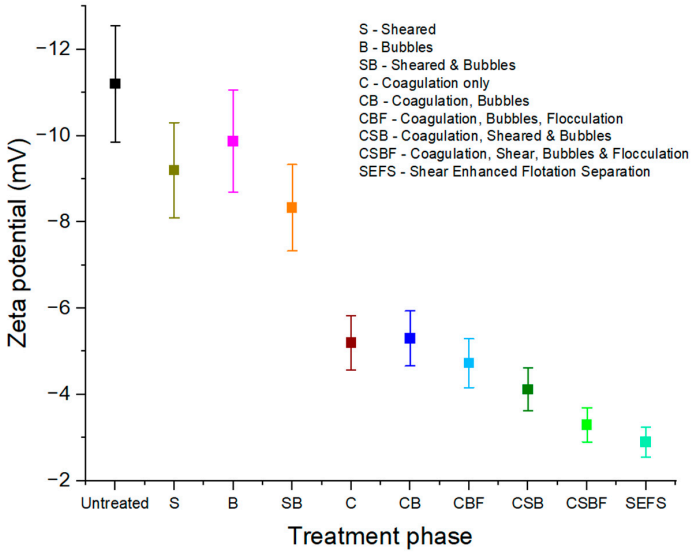

Figure 6. Zeta potential as a function of treatment phase.

The zeta potential as a function of treatment displayed a general trend where each successive treatment phase affected the surface charge of the particles. The raw/untreated wastewater displayed zeta potential values of −11.4 mV. When exposed to shear, the average zeta potential observed for the solution was −9.1 mV, (a 19% change in zeta potential). In contrast, when bubbles were used, the zeta potential was observed to increase to −9.8 mV (become more negative). The observed negative zeta potential of the microbubbles in water can be attributed to the adsorption of OH^- ions at the interface of the bubbles, originating from the water molecules [60]. Microbubbles have a comparatively elevated zeta potential, and empirical findings indicate that the pronounced negative charge of microbubbles restricts their coalescence. Consequently, the structural integrity of the bubbles is preserved at various depths and can remain intact for prolonged durations [61].

The introduction of the coagulant caused the zeta potential to change significantly from −8.2 mV with shearing and bubbles (in absence of coagulant) to −5.4 mV (after coagulation). This change in zeta potential is attributed to the positive counterions added during coagulation, which induces adsorption of ions and subsequent neutralization of surface charges. Conventional DAF samples labelled in Figure 6 as CBF (coagulation, bubbles, and flocculation) caused surface charge reduction to −4.2 mV. These samples were taken from SP-3. The CSBF (coagulation, shear, bubbles, and flocculation)), as denoted in Figure 6, relates to the post-treatment and was taken via the recycle sample line (SP-4). The SEFS samples, on the other hand, were taken directly from the DAF tank exit point (SP-3).

Synergistic effects of shear, coagulation, flocculation, and flotation (SEFS/CSBF) collectively enhanced the overall destabilization of colloidal particles in the wastewater in comparison to conventional DAF treatment (CBF).

3.5. Influence of Microbubbles

Many researchers have debated the definition of microbubble sizes. For example, Agarwal et al. (2011), described these as small bubbles with sizes ranging from 10 to 50 µm [62]. Interestingly, Takahashi et al. (2007) classified these particular bubbles as having diameters less than 50 µm [63]. In a separate investigation by Terasaka et al. (2011), the microbubbles were categorized as small bubbles, with dimensions ranging from 10 to 60 µm, according to their specific field of use within a study examining physiological activity [64].

Relating the bubble size presented in Figure 7 to the particle size in Figure 5, it can be inferred that the separation process was more effective when the bubble size and the

particle size are in the same order of magnitude. For example, the average bubble size of the conventional DAF treatment was 126 µm. In comparison, that of the SEFS-treated wastewater was 62 µm. The shear unit creates a highly turbulent environment and increases the collision probability between colloids and bubbles, which enhances the solid/liquid separation process as opposed to that without shearing in conventional DAF treatment. By increasing the collision frequency between bubbles and particles and capture efficiencies, greater separation efficiencies can be achieved [65].

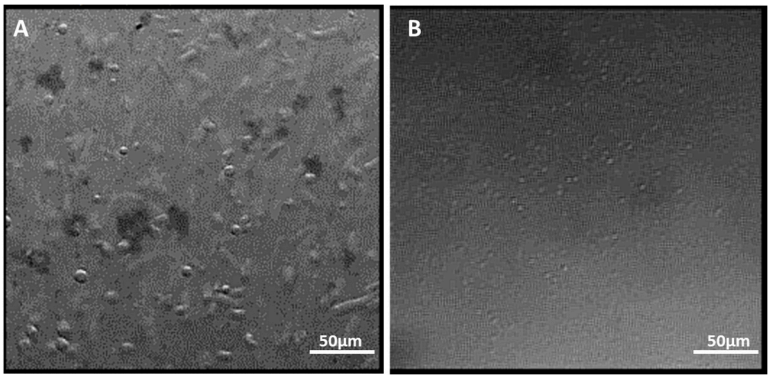

Figure 7. Snapshot of bubble size analysis of (**A**) conventional DAF and (**B**) SEFS treatment.

A total of 1456 bubbles were quantified, and the different bubble size bins are illustrated in Figure 8. The mean conventional DAF bubble size (Figure 8A) fell within the bin range of 50–150 µm, representing roughly 60% of the bubble's sizes. According to various literature studies, these bubble sizes are well within the reported range for DAF treatment of wastewater [66–68]. When the wastewater was exposed to hydrodynamic shear (Figure 8B), the frequency of smaller microbubbles was observed to increase. The bubble size in the range 50–100 µm was 30% more with shear treatment than conventional DAF treatment. Furthermore, unlike the DAF-treated wastewater, the SEFS treatment generated bubbles with sizes less than 50 µm. The enhancement in the frequency and quantity smaller bubbles (<100 µm) may therefore explain the higher removal efficiencies when using hydrodynamic shear as a component during winery wastewater treatment. Wu et al. (2015) similarly stated that smaller gas bubbles and their ability to increase the contact area (spreading of the gas bubble on the particle) creates an environment where the hydrodynamic disruptive shear force remains stable [69]. In other words, microbubbles induced by hydrodynamic shear selectively attach to micron-size particles while still keeping their mechanical strength and integrity.

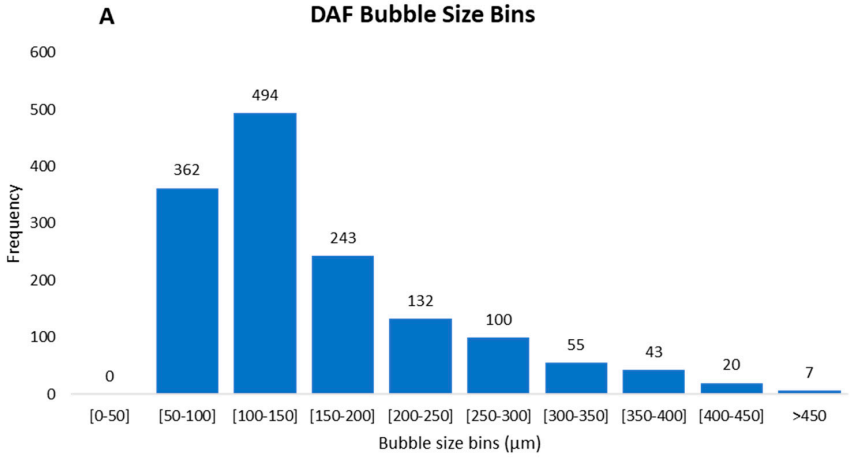

Figure 8. *Cont.*

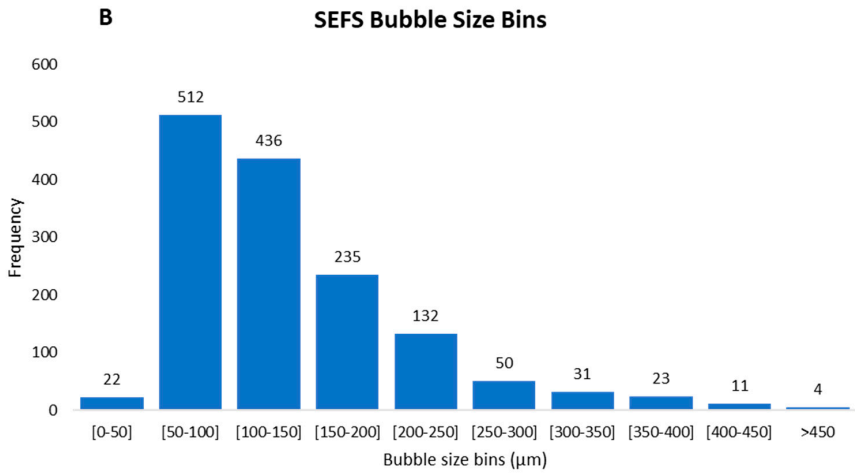

Figure 8. Histogram of bubble sizes for (**A**) conventional DAF- and (**B**) SEFS-treated wastewater.

The beneficial nature of the smaller-sized microbubbles generated using the shear mixer stems from its ability to offer a larger particle surface area, which enhances the attachment of particles to the bubbles and facilitates the buoyancy of the suspended solids. Research findings indicate that a clear correlation exists between the necessity to decrease bubble size and the heightened likelihood of collisions occurring between bubbles and particles [70]. The importance of bubble size and particle size in relation to treatment efficiency is evident during turbidity and total suspended solids studies, as discussed in the following section.

3.6. Turbidity and Total Suspended Solids

Figure 9 illustrates turbidity values as a function of treatment phase. Turbidity refers to the measurement of the relative transparency of a liquid and quantifies the optical property of water. More specifically, it is the quantification of light scattering caused by the presence of particulate matter within a water sample when illuminated by a light source. High concentrations of particulate matter affect light penetration, subsequently leading to elevated turbidity values.

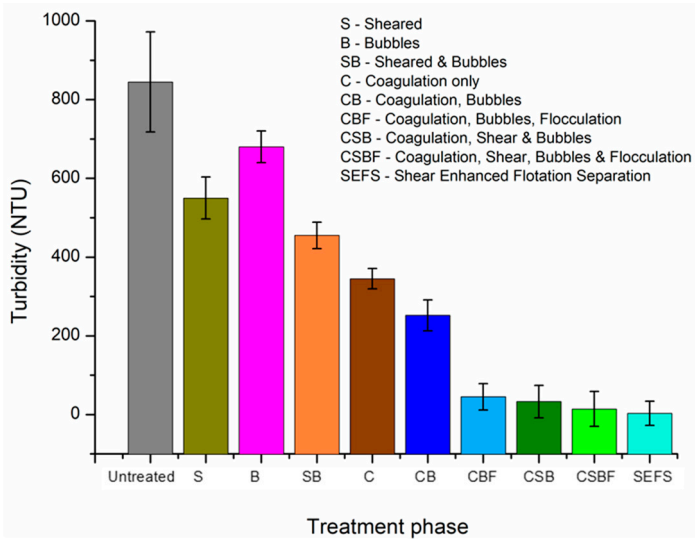

Figure 9. Turbidity studies as a function of treatment phase.

Turbidity values depicted in Figure 9 show that with each treatment phase, the turbidity systematically decreased, with untreated wastewater having turbidity of 849 NTU, whereas the final (SEFS) treated wastewater had values similar to that of drinking water

(3 NTU). The slight increase in turbidity for the samples only exposed to bubbles (labelled as B in Figure 9) can be explained by the flotation mechanism free of chemical additives, disturbing the solution equilibrium, which leads to a higher degree of suspended particles in solution.

Table 3 shows the TSS and turbidity treatment values of the wastewater and compares the difference between conventional DAF treatment and the addition of shear during SEFS treatment.

Table 3. Total suspended solids (TSS) and turbidity values of wastewater at different stages of treatment.

Sample Type	TSS (mg/L)		Turbidity (NTU)	
	Conventional DAF	SEFS	Conventional DAF	SEFS
Untreated	2620	2620	849	849
Treated	75	17	35	3
% Treatment efficiency (treated vs. untreated)	97.1	99.4	95.8	99.6

The data presented in Table 3 illustrate that a significant reduction in both TSS and turbidity was achieved with both treatment methods. However, when exposed to shear, the treatment efficiency increased for both TSS and turbidity quality parameters. These values are further complemented with the visual differences in haziness as depicted in Figure 10. Although the treatment efficiencies of both treatment systems may seem relatively similar, it should be noted that the TSS in wastewater to be used as irrigation water must be below 25 mg/L. Based on the TSS values, it can be concluded that SEFS-treated wastewater would meet these minimum requirements.

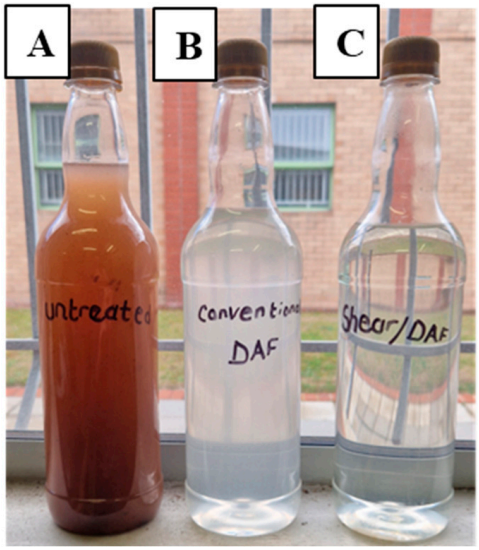

Figure 10. Visual comparison between (**A**) untreated, (**B**) conventional DAF-, and (**C**) SEFS-treated wastewater.

3.7. Chemical Oxygen Demand

The efficacy of the DAF and SEFS treatment was evaluated by assessing capacity to decrease chemical oxygen demand before and after treatment, as depicted in Figure 11. The chemical oxygen demand (COD) of the wastewater treated with conventional DAF displayed values of 5490 mg/L with initial COD for the untreated wastewater having a value of 11,140 mg/L. The SEFS-treated wastewater resulted in a significant reduction of 66%, decreasing from an initial concentration of 11,140 mg/L to 3800 mg/L.

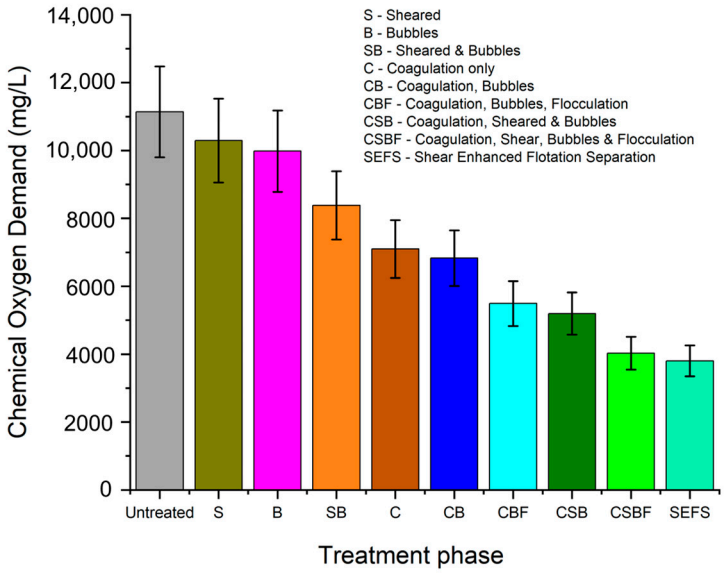

Figure 11. Chemical oxygen demand as a function of treatment stages.

The difference in COD reduction between the two treatment methods may be attributed to the increased agglomeration of particles as well as the smaller bubbles generated during shear, which creates a higher collision probability between bubbles and particles. The greater frequency of microbubbles in the range 0–100 μm additionally allowed for an increase in flotation and solid/liquid separation as opposed to conventional DAF treatment.

The positive results, particularly in terms of suspended solids and turbidity, can primarily be attributed to the synergistic effects of the enhanced particle destabilization process and the flotation phenomenon. However, it is worth noting that the impact on COD levels appears to be less pronounced than on the TSS and turbidity. The SEFS procedure effectively eliminates a significant portion of the particulate COD component, as demonstrated by the data presented in Table 4. Hence, the relatively lower percentage decrease in COD in comparison to an average of 96% reduction in TSS and turbidity, respectively, for conventional DAF and an average of 99% reduction in TSS and turbidity for SEFS-treated wastewater is likely attributable to the residual dissolved organic compounds present in the wastewater.

Table 4. COD values of wastewater at different stages of treatment.

Sample Type	COD (mg/L)	
	Conventional DAF	**SEFS**
Untreated	11,140	11,140
Treated	5490	3800
% Treatment efficiency (untreated vs. treated)	51	66

A review was conducted by Ioannou et al. (2015) where several primary physicochemical winery wastewater treatment methods were evaluated [26]. These included chemical precipitation with chelating agents, coagulation/flocculation, electrocoagulation, and sedimentation. Amongst these treatment methods, the average COD removal rates for winery wastewater was generally less than 45%. One exception was the implementation of chitosan as a natural coagulant, where 73% of COD was removed [26].

A comparison between chemical requirements with and without shear is presented in Table 5. The differences observed can be explained by the different mechanisms of aggregation. During conventional DAF treatment, the aggregation is governed by the

Brownian motion of the particles (perikinetic aggregation). In contrast, the formation of aggregates when an external flow field is applied, such as shear mixing, produces orthokinetic aggregates. Orthokinetic aggregation has been shown to enhance the aggregation rate of colloids compared to Brownian mechanisms [71]. Furthermore, hydrodynamic shearing has the advantage of intensifying chemical reaction processes with fast inherent reaction rates but relatively slow mass transfer rates [72].

Table 5. Chemical requirements: conventional DAF versus SEFS.

Parameter	Conventional DAF	SEFS	% Difference
Shear speed (RPM)	0	3250	-
Coagulant concentration (ppm)	4.4	2.8	36.4
Flocculant concentration (ppm)	10.3	7.1	31.1

Cagnetta et al. (2019) conducted a study to evaluate the efficacy of dissolved air flotation (DAF) in combination with a pilot-scale high-speed activated sludge system at the municipal water treatment plant in Aartselaar, Belgium. Following activated sludge and DAF treatment, their findings indicated a reduction of 78% in TSS and 68% in COD [73]. In comparison, the results of our study indicate that SEFS treatment caused a significant reduction in COD of 66% compared to 51% using conventional DAF treatment, without using any other additional technologies (such as activated sludge in the mentioned study by Cagnetta et al. (2019). Our findings suggest that SEFS treatment holds promise as a viable and efficient method for treating winery wastewater to appropriate discharge levels. SEFS technology exhibits promising potential for upscaling, as seen by its effective COD reduction and high reduction values for turbidity and total suspended solids. This suggests that SEFS technology could be successfully implemented on a larger scale, particularly in conjunction with a secondary treatment stage such as membrane bioreactors.

3.8. Froth Analysis

The general process of DAF treatment produces various quantities of froth. In the process of dissolved air flotation, the initial step involves pressure to achieve air saturation. Subsequently, the water that has reached its saturation point undergoes pressure release to atmospheric level, leading to the creation of microbubbles [74]. The introduction of microbubbles in the flotation tank facilitates their interaction with the contaminants present in the water. Ultimately, the bubbles become affixed to the contaminants and ascend to the water's surface, forming a foam comprising complexes composed of bubbles and pollutants. This froth should theoretically consist of a vast majority of the particulate material that was floated during winery wastewater processing. A dense and concentrated form of froth that was generated is shown in Figure 12.

Figure 12. Froth produced during SEFS treatment process.

The soil used by the winery in our case study mostly contains sand and 1% stone. At a depth of 30cm, the soil has a pH of 6.1 and is saturated with Na (5.6%), K (3.5%), Ca (45.9%), and Mg (20%). As with any crop, grapevine development and output depend on proper nutrition. The primary nutrient influencing grapevine health and quality is nitrogen. The incorporation of potassium has been found to enhance grape productivity, primarily by enhancing both grape cluster quantity and weight [75]. Both calcium and magnesium are essential nutrients, required for optimal grapevine performance. Generally, these nutrients are abundant in soils with pH values within the optimal range, making fertilization of these nutrients unnecessary [76]. However, in order to consistently produce grapes of high quality, fertilizers are primarily used in agriculture. One of the aims of this research was to investigate the contents of the froth to determine its potential suitability for use as fertilizer. Table 6 displays the characteristics of macronutrients and micronutrients in the froth as well as that of a commercially available fertilizer.

Table 6. Macronutrient chemical composition of froth and commercial fertilizer.

Element	Unit of Measurement	Conventional DAF	SEFS	Commercial Fertilizer
Ca	(%)	1.7	1.9	8.2
Mg	(%)	3.1	3.4	5.7
S	(%)	7.9	7.8	8.1
N	(%)	6.1	5.8	17.1
P	(%)	4.2	3.9	14.2
K	(%)	2.6	2.8	18.5
Fe	mg/kg	79.1	87.6	950
Cu	mg/kg	6.7	6.5	13.2
Zn	mg/kg	13.3	13.1	117
Mn	mg/kg	30.8	36.1	220
B	mg/kg	5.8	8.9	242
Mo	mg/kg	3.5	4.2	6.5

The values depicted in Table 6 suggest that regardless of adding shear to the treatment process, the nutrient composition of the froth remained chemically similar. In comparison, the pilot plant treated water does not meet the minimum requirements for the solid waste to be used as fertilizer in its current state. A study was conducted by Conradie et al. (2020) that investigated the annual nutrient requirements to produce 30 tons of grapes per hectare in South Africa [76]. Their results demonstrated that macronutrients (N, P, K, Ca, and Mg) required to produce one ton of grapes are (N) 3.93 kg/ha, 0.7 kg/ha (P), 3.2 kg/ha (K), 2.77 kg/ha (Ca), and 0.77 kg/ha (Mg). Our froth analysis results in Table 6 showed the presence of important macronutrients for crop growth albeit in small percentages in comparison to commercial fertilizer. The breakdown of this organic matter in the soil releases nutrients that plants may absorb, such as potassium, phosphate, and nitrogen, which lowers the amount of fertilizer needed by the vines. Based on the macronutrient content in the froth, it may be feasible to mix the dried froth with commercial fertilizer to reduce solid waste disposal expenses and potentially decrease vineyard running costs. Micronutrients, on the other hand, are mineral elements required in small quantities (expressed in mg/kg) by plants for normal growth and development. The froth displayed micronutrient concentrations much lower than those found in commercial fertilizer [76]. Based on the nutrients presented in Table 6, it may be inferred that froth application to soil may not cause detrimental harm. The effects of adding dried foam to the soil will, however, need to be investigated in a future study.

3.9. Pilot Plant Energy Requirements and Cost to Treat Winery Wastewater

The treatment efficiency of both conventional DAF as well as SEFS are discussed in Sections 3.6 and 3.7. Although promising efficiency results are reported, it is important to evaluate the energy requirements to treat winery wastewater using these two systems.

Table 7 illustrates the values associated to the power consumption of each parameter during treatment.

Table 7. Energy consumption during wastewater treatment.

	Power Consumption (kWh/m^3)
Inlet pump	0.032
Coagulant dosing pump	0.048
Flocculant dosing pump	0.076
Microbubble generator	0.418
Shear mixer	0.478
Outlet pump	0.034

The energy consumed to treat 1 m^3 of winery wastewater using conventional DAF amounted to roughly 0.6 kWh/m^3 whereas the SEFS treatment energy was 1.1 kWh/m^3, as also illustrated in Figure 13. Although the energy requirement during SEFS treatment is over 1.5 times that of conventional DAF treatment, the quality of the treated wastewater may outweigh the overall energy costs, as shown in Table 8.

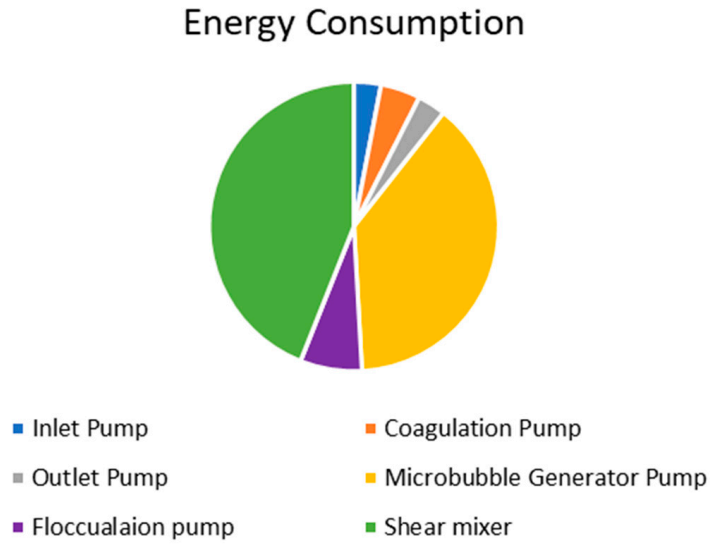

Figure 13. Energy consumption SEFS treatment process.

Table 8. Material and operational costs to treat 1 m^3 of effluent.

Material and Operational Costs			
	Units	DAF	SEFS
Energy consumed	kWh/m^3	0.6	1.1
Coagulant	ZAR/m^3	R0.86	R0.37
Flocculant	ZAR/m^3	R0.34	R0.13
Energy cost in ZAR	ZAR */kWh	R1.08	R1.98
Energy cost in US dollars	USD **/kWh	$0.055	$0.063
Treatment Efficiency			
TSS	%	97.1	99.4
Turbidity	%	95.8	99.6
COD	%	51	66

* ZAR (South African rand). ** Current ZAR to US dollar exchange rate at time of publication.

Table 8 illustrates the operational and materials costs during the treatment of 1 m^3 of effluent. Based on the results obtained, specifically the treatment efficiencies, the additional energy input costs of the SEFS treatment system are therefore deemed to be justifiable.

More specifically, the results highlight the cost saving during chemical treatment with SEFS. As such, wineries that consider SEFS treatment may potentially save on cumulative energy costs (e.g., biological treatment) as well as general wastewater discharge costs.

4. Conclusions

This study focused on the design and application of a hybrid shear enhanced flotation separation (SEFS) treatment plant to process winery wastewater. Our study comprised the individual and synergistic effects of chemical additives and microbubbles, with and without shear. To our knowledge, this is the one of the first studies where hydrodynamic shear as a treatment component has been implemented during winery wastewater treatment. It has been shown that hydrodynamic shear as a component enhances overall treatment efficiency. The energy consumption for DAF treatment was 0.6 kWh/m^3, whereas that of SEFS treatment was 1.1 kWh/m^3. The nearly twofold increase in energy consumed was, however, justified by the total operational and energy costs to treat 1 m^3 of wastewater. A 99.6% and 99.4% reduction in turbidity (a decrease from 849 NTU to 3 NTU) and TSS (a decrease from 2620 mg/L to 17 mg/L), respectively, was achieved through SEFS treatment in comparison to the 95.8% and 97.1% reduction in turbidity (a decrease from 849 NTU to 35 NTU) and TSS (2620 mg/L to 75 mg/L), respectively, achieved with conventional DAF. Chemical oxygen demand values were reduced by 66% (from 11,140 mg/L to 3800 mg/L) using the SEFS treatment system. Comparatively, a reduction of 51% for the COD was obtained using the conventional DAF treatment system (from 11,140 mg/L to 5490 mg/L). Not only was it shown that shear enhances treatment efficiency, but this technology also required 33% less coagulant and 37% less flocculant compared to conventional DAF treatment.

Solid waste analyses showed that the froth generated during the treatment process may be considered as a suitable source of fertilizer based on the nutrients contained therein. Before this solid waste can be considered for mixing with commercial fertilizer, the harmful/beneficial properties of the froth towards soil application should be thoroughly investigated.

The feasibility of SEFS technology to successfully treat agricultural wastewater has thus been shown and may also be applied to treat other wastewater types (e.g., pharmaceutical and municipal). This study showed a substantial reduction in COD; however, the remaining COD concentration in the wastewater is ascribed to the soluble fraction, which could not be removed using SEFS technology. The fraction of soluble COD is typically considered to be highly biodegradable due to the existence of easily biodegradable compounds such as simple sugars and disaccharides. Thus, future studies will include the further treatment of and reduction in soluble COD by means of biological treatment.

Author Contributions: Conceptualization, D.V. and B.J.B.; methodology, D.V.; formal analysis, D.V., writing—original draft preparation, D.V.; writing—review and editing, D.V., B.J.B., B.C. and D.K.; supervision, B.J.B. and D.K.; funding acquisition, B.J.B. All authors have read and agreed to the published version of the manuscript.

Funding: This research was funded by Winetech, project number UWC BB-20-01.

Data Availability Statement: Data are contained within the article.

Acknowledgments: This study was conducted as a component of a doctoral research dissertation at the South African Institute of Advanced Materials Chemistry, University of Western Cape, South Africa. The authors would like to extend their gratitude to all individuals who aided in the execution of this study. The authors express their sincere gratitude to the technical team at the winery for their assistance and invaluable help during the duration of this study.

Conflicts of Interest: The authors declare no conflict of interest. The funders did not contribute to this study's design, data collection, analysis, interpretation, manuscript writing, or the decision to publish the findings.

References

1. Oliveira, M.; Duarte, E. Integrated Approach to Winery Waste: Waste Generation and Data Consolidation. *Front. Environ. Sci. Eng.* **2016**, *10*, 168–176. [CrossRef]
2. Mosse, K.P.; Vincent Verheyen, T.; Cruickshank, A.J.; Patti, A.F.; Cavagnaro, T.R. Thermochemolysis of Winery Wastewater Particulates—Molecular Structural Implications for Water Reuse. *J. Anal. Appl. Pyrolysis* **2012**, *97*, 164–170. [CrossRef]
3. Christ, K.L.; Burritt, R.L. Critical Environmental Concerns in Wine Production: An Integrative Review. *J. Clean. Prod.* **2013**, *53*, 232–242. [CrossRef]
4. Broome, J.; Warner, K. Agro-Environmental Partnerships Facilitate Sustainable Wine-Grape Production and Assessment. *Calif. Agric.* **2008**, *62*, 133–141. [CrossRef]
5. Lauzurique, Y.; Espinoza, L.C.; Huiliñir, C.; García, V.; Salazar, R. Anodic Oxidation of Industrial Winery Wastewater Using Different Anodes. *Water* **2022**, *14*, 95. [CrossRef]
6. Kookana, R.; Kumar, A. *Impact of Winery Wastewater on Ecosystem Health—An Introductory Assessment*; CSIRO: Adelaide, Australia, 2006.
7. Vinpro Expects 2023 Wine Grape Season to Deliver "Excellent" Wines. Available online: https://www.engineeringnews.co.za/article/vinpro-expects-2023-wine-grape-season-to-deliver-excellent-wines-2023-05-17 (accessed on 12 June 2023).
8. SAWIS. *South African Wine Harvest Report*; SAWIS: Paarl, South Africa, 2020.
9. Wine Australia. *National Vintage Report 2022*; Wine Australia: Canberra, Australia, 2022.
10. California Department of Food and Agriculture. *California Grape Crush Report 2022*; California Department of Food and Agriculture: Sacramento, CA, USA, 2022.
11. Ahmadi, L.; Merkley, G.P. Wastewater Reuse Potential for Irrigated Agriculture. *Irrig. Sci.* **2017**, *35*, 275–285. [CrossRef]
12. Zeng, Z.; Liu, J.; Savenije, H.H.G. A Simple Approach to Assess Water Scarcity Integrating Water Quantity and Quality. *Ecol. Indic.* **2013**, *34*, 441–449. [CrossRef]
13. Devesa-rey, R.; Vecino, X.; Varela-alende, J.L.; Barral, M.T.; Cruz, J.M.; Moldes, A.B. Valorization of Winery Waste vs. the Costs of Not Recycling. *Waste Manag.* **2011**, *31*, 2327–2335. [CrossRef]
14. Smagghe, F.; Mourgues, J.; Escudier, J.L.; Conte, T.; Molinier, J.; Malmary, C. Recovery of Calcium Tartrate and Calcium Malate in Effluents from Grape Sugar Production by Electrodialysis. *Bioresour. Technol.* **1992**, *39*, 185–189. [CrossRef]
15. Conradie, A.; Sigge, G.O.; Cloete, T.E. Influence of Winemaking Practices on the Characteristics of Winery Wastewater and Water Usage of Wineries. *S. Afr. J. Enol. Vitic.* **2014**, *35*, 10–19. [CrossRef]
16. Mulidzi, A.; Clarke, C.; Myburgh, P. Annual Dynamics of Winery Wastewater Volumes and Quality and the Impact of Disposal on Poorly Drained Duplex Soils. *S. Afr. J. Enol. Vitic.* **2018**, *39*, 305–314. [CrossRef]
17. Melamane, X.L.; Strong, P.J.; Burgess, J.E. Treatment of Wine Distillery Wastewater: A Review with Emphasis on Anaerobic Membrane Reactors. *S. Afr. J. Enol. Vitic.* **2007**, *28*, 25–36. [CrossRef]
18. Bustamante, M.A.; Moral, R.; Paredes, C.; Pe, A.; Pe, M.D. Agrochemical Characterisation of the Solid By-Products and Residues from the Winery and Distillery Industry. *Waste Manag.* **2008**, *28*, 372–380. [CrossRef] [PubMed]
19. Shepherd, H.L.; Grismer, M.E.; Tchobanoglous, G. Treatment of High-strength Winery Wastewater Using a Subsurface-flow Constructed Wetland. *Water Environ. Res.* **2001**, *73*, 394–403. [CrossRef]
20. Mosse, K.P.M.; Patti, A.F.; Christen, E.W.; Cavagnaro, T.R. Review: Winery Wastewater Quality and Treatment Options in Australia. *Aust. J. Grape Wine Res.* **2011**, *17*, 111–122. [CrossRef]
21. Bolognesi, S.; Cecconet, D.; Capodaglio, A.G. 5—Agro-Industrial Wastewater Treatment in Microbial Fuel Cells. In *Integrated Microbial Fuel Cells for Wastewater Treatment*; Abbassi, R., Yadav, A.K., Khan, F., Garaniya, V., Eds.; Butterworth-Heinemann: Oxford, UK, 2020; pp. 93–133; ISBN 978-0-12-817493-7.
22. Chatzilazarou, A.; Gortzi, O.; Lalas, S.; Katsoyannos, E. Removal of Polyphenols from Wine Sludge Using Cloud Point Extraction. *J. Air Waste Manag. Assoc.* **2010**, *60*, 454–459. [CrossRef]
23. Teh, C.Y.; Budiman, P.M.; Shak, K.P.Y.; Wu, T.Y. Recent Advancement of Coagulation-Flocculation and Its Application in Wastewater Treatment. *Ind. Eng. Chem. Res.* **2016**, *55*, 4363–4389. [CrossRef]
24. Sohrabi, Y.; Rahimi, S.; Nafez, A.H.; Mirzaei, N.; Bagheri, A.; Ghadiri, S.K.; Rezaei, S.; Charganeh, S.S. Chemical Coagulation Efficiency in Removal of Water Turbidity. *Int. J. Pharm. Res.* **2018**, *10*, 188–194. [CrossRef]
25. Amor, C.; Lucas, M.S.; Pirra, A.J.; Peres, J.A.; Santo, C.E.; Vilar, V.J.P.; Botelho, C.M.S.; Bhatnagar, A.; Kumar, E.; Boaventura, R.A.R.; et al. Coagulation-Flocculation Mechanisms in Wastewater Treatment Plants through Zeta Potential Measurements. *S. Afr. J. Enol. Vitic.* **2022**, *51*, 1–10. [CrossRef]
26. Ioannou, L.A.; Puma, G.L.; Fatta-Kassinos, D. Treatment of Winery Wastewater by Physicochemical, Biological and Advanced Processes: A Review. *J. Hazard. Mater.* **2015**, *286*, 343–368. [CrossRef]
27. Vlotman, D.E.; Key, D.; Bladergroen, B.J. Technological Advances in Winery Wastewater Treatment: A Comprehensive Review. *S. Afr. J. Enol. Vitic.* **2022**, *43*, 58–80. [CrossRef]
28. Lucas, M.S.; Peres, J.A.; Li Puma, G. Treatment of Winery Wastewater by Ozone-Based Advanced Oxidation Processes (O3, O3/UV and O3/UV/H2O2) in a Pilot-Scale Bubble Column Reactor and Process Economics. *Sep. Purif. Technol.* **2010**, *72*, 235–241. [CrossRef]
29. Bolzonella, D.; Papa, M.; Da Ros, C.; Anga Muthukumar, L.; Rosso, D. Winery Wastewater Treatment: A Critical Overview of Advanced Biological Processes. *Crit. Rev. Biotechnol.* **2019**, *39*, 489–507. [CrossRef] [PubMed]

30. Cerff, B.R. *Effluent Water Treatment Utilising a Combination of Hydrodynamic Shear and Flotation Technology for the Specific Application of Wastewater from the Oil and Gas Industry*; University of the Western Cape: Cape Town, South Africa, 2022.
31. Crini, G.; Lichtfouse, E. Advantages and Disadvantages of Techniques Used for Wastewater Treatment. *Environ. Chem. Lett.* **2019**, *17*, 145–155. [CrossRef]
32. Shardt, O.; Derksen, J.J.; Mitra, S.K. Simulations of Droplet Coalescence in Simple Shear Flow. *Langmuir* **2013**, *29*, 6201–6212. [CrossRef] [PubMed]
33. Zhang, J.; Xu, S.; Li, W. High Shear Mixers: A Review of Typical Applications and Studies on Power Draw, Flow Pattern, Energy Dissipation and Transfer Properties. *Chem. Eng. Process. Process. Intensif.* **2012**, *57–58*, 25–41. [CrossRef]
34. Russel, W.B.; Saville, D.A.; Schowalter, W.R. Colloidal Dispersions. *J. Fluid Mech.* **1989**, *222*, 525–582. [CrossRef]
35. Deshawar, D.; Kumar, V. Hydrodynamics and Mixing Characterization in a Novel High Shear Mixer. *Chem. Eng. Process. Process Intensif.* **2017**, *120*, 57–67. [CrossRef]
36. Rulyov, N.N. Combined Microflotation of Fine Minerals: Theory and Experiment. *Trans. Institutions Min. Metall. Sect. C Miner. Process. Extr. Metall.* **2016**, *125*, 81–85. [CrossRef]
37. Rajak, V.K.; Relish, K.K.; Kumar, S.; Mandal, A. Mechanism and Kinetics of Separation of Oil from Oil-in-Water Emulsion by Air Flotation. *Pet. Sci. Technol.* **2015**, *33*, 1861–1868. [CrossRef]
38. Spicer, P.T.; Pratsinis, S.E. Coagulation and Fragmentation: Universal Steady-State Particle-Size Distribution. *AIChE J.* **1996**, *42*, 1612–1620. [CrossRef]
39. Wei, N.; Zhang, Z.; Liu, D.; Wu, Y.; Wang, J.; Wang, Q. Coagulation Behavior of Polyaluminum Chloride: Effects of PH and Coagulant Dosage. *Chin. J. Chem. Eng.* **2015**, *23*, 1041–1046. [CrossRef]
40. Peter, G. Using Polyaluminium Coagulants in Water Treatment. In Proceedings of the 64th Annual Water Industry Engineers and Operators' Conference, Bendigo, Australia, 5–6 September 2001; pp. 39–47.
41. Ukiwe, L.N.; Alinnor, J.I. Assessment of Polyacrylamide and Aluminum Sulphate Coagulants in Turbidity Removal in Wastewater. *Terr. Aquat. Environ. Toxicol.* **2012**, *6*, 132–135.
42. Vanni, M.; Baldi, G. Coagulation Efficiency of Colloidal Particles in Shear Flow. *Adv. Colloid Interface Sci.* **2002**, *97*, 151–177. [CrossRef]
43. Jarvis, P.; Jefferson, B.; Parsons, S.A. Floc Structural Characteristics Using Conventional Coagulation for a High Doc, Low Alkalinity Surface Water Source. *Water Res.* **2006**, *40*, 2727–2737. [CrossRef]
44. Vlotman, D.; Key, D.; Cerff, B.; Bladergroen, B.J. Shear Enhanced Flotation Separation Technology in Winery Wastewater Treatment. *Water* **2023**, *15*, 2409. [CrossRef]
45. Cerff, B.R.; Bladergroen, B.; Jansen, P. Recovery of Uncontaminated Oils from Emulsions Based on Mechanically Induced Flocculation of Stable Emulsions. Patent Application 2023/07437, 15 November 2022. University of the Western Cape Technology Transfer Office.
46. Mulidzi, A.R. The Effect of Winery Wastewater Irrigation on the Properties of Selected Soils from the South African Wine Region. Ph.D. Thesis, Stellenbosch University, Stellenbosch, South Africa, 2016.
47. Alhelí, J.; Torrejón, A.; Balderas, P.; Gabriela, H.; Morales, R. Relationship, Importance, and Development of Analytical Techniques: COD, BOD and TOC in Water—An Overview through Time. *SN Appl. Sci.* **2023**, *5*, 118. [CrossRef]
48. Malvern Instruments Limited. *Zeta Potential: An Introduction in 30 Minutes*; Malvern Instruments, Ltd.: Oxford, UK, 2011; Volume 2.
49. *ASTMD5907-18*; Standard Test Method for Filterable and Nonfilterable Matter in Water. ASTM International: West Conshohocken, PN, USA, 2018; Volume 18.
50. Schneider, C.A.; Rasband, W.S.; Eliceiri, K.W. NIH Image to ImageJ: 25 Years of Image Analysis. *Nat. Methods* **2012**, *9*, 671–675. [CrossRef]
51. Holtman, G.A.; Haldenwang, R.; Welz, P.J. Biological Sand Filter System Treating Winery Effluent for Effective Reduction in Organic Load and PH Neutralisation. *J. Water Process. Eng.* **2018**, *25*, 118–127. [CrossRef]
52. Duarte, J.C.; Federici, F.; Lellk, V.S.C. De High-Rate Aerobic Treatment of Winery Wastewater Using Bioreactors with Free and Immobilized Activated Sludge. *J. Biosci. Bioeng.* **2000**, *90*, 381–386.
53. Skornia, K.; Safferman, S.I.; Rodriguez-Gonzalez, L.; Ergas, S.J. Treatment of Winery Wastewater Using Bench-Scale Columns Simulating Vertical Flow Constructed Wetlands with Adsorption Media. *Appl. Sci.* **2020**, *10*, 1063. [CrossRef]
54. Ioannou, L.A.; Michael, C.; Vakondios, N.; Drosou, K.; Xekoukoulotakis, N.P.; Diamadopoulos, E.; Fatta-Kassinos, D. Winery Wastewater Purification by Reverse Osmosis and Oxidation of the Concentrate by Solar Photo-Fenton. *Sep. Purif. Technol.* **2013**, *118*, 659–669. [CrossRef]
55. Department of Water Affairs. *Revision of General Authorisations in Terms of Section 39 of the National Water Act, 1998 (Act No. 36 of 1998), No. 665. Government Gazette No. 36820, 6 September 2013*; Department of Water Affairs: Pretoria, South Africa, 2013.
56. Bałdyga, J.; Orciuch, W.; Makowski, Ł.; Malski-Brodzicki, M.; Malik, K. Break up of Nano-Particle Clusters in High-Shear Devices. *Chem. Eng. Process. Process. Intensif.* **2007**, *46*, 851–861. [CrossRef]
57. Dogon, D.; Golombok, M. Particle Agglomeration in Sheared Fluids. *J. Pet. Explor. Prod. Technol.* **2015**, *5*, 91–98. [CrossRef]
58. Mishra, V.; Kresta, S.M.; Masliyah, J.H. Self-Preservation of the Drop Size Distribution Function and Variation in the Stability Ratio for Rapid Coalescence of a Polydisperse Emulsion in a Simple Shear Field. *J. Colloid Interface Sci.* **1998**, *197*, 57–67. [CrossRef]
59. Předota, M.; Machesky, M.L.; Wesolowski, D.J. Molecular Origins of the Zeta Potential. *Langmuir* **2016**, *32*, 10189–10198. [CrossRef]

60. Temesgen, T.; Bui, T.T.; Han, M.; Kim, T.; Park, H. Micro and Nanobubble Technologies as a New Horizon for Water-Treatment Techniques: A Review. *Adv. Colloid Interface Sci.* **2017**, *246*, 40–51. [CrossRef]
61. Edzwald, J.K. Dissolved Air Flotation and Me. *Water Res.* **2010**, *44*, 2077–2106. [CrossRef]
62. Agarwal, A.; Ng, W.J.; Liu, Y. Principle and Applications of Microbubble and Nanobubble Technology for Water Treatment. *Chemosphere* **2011**, *84*, 1175–1180. [CrossRef]
63. Takahashi, M.; Chiba, K.; Li, P. Free-Radical Generation from Collapsing Microbubbles in the Absence of a Dynamic Stimulus. *J. Phys. Chem. B* **2007**, *111*, 1343–1347. [CrossRef]
64. Terasaka, K.; Hirabayashi, A.; Nishino, T.; Fujioka, S.; Kobayashi, D. Development of Microbubble Aerator for Waste Water Treatment Using Aerobic Activated Sludge. *Chem. Eng. Sci.* **2011**, *66*, 3172–3179. [CrossRef]
65. Chin, C.J.; Yiacoumi, S.; Tsouris, C. Shear-Induced Flocculation of Colloidal Particles in Stirred Tanks. *J. Colloid Interface Sci.* **1998**, *206*, 532–545. [CrossRef] [PubMed]
66. Palaniandy, P.; Adlan, H.; Aziz, H.; Murshed, M.; Hung, Y. *Dissolved Air Flotation (DAF) for Wastewater Treatment*; CRC Press: Boca Raton, FL, USA, 2017; ISBN 9781315164199.
67. El-Gohary, F.; Tawfik, A.; Mahmoud, U. Comparative Study between Chemical Coagulation/Precipitation (C/P) versus Coagulation/Dissolved Air Flotation (C/DAF) for Pre-Treatment of Personal Care Products (PCPs) Wastewater. *Desalination* **2010**, *252*, 106–112. [CrossRef]
68. Kyzas, G.Z.; Matis, K.A. Flotation in Water and Wastewater Treatment. *Processes* **2018**, *6*, 116. [CrossRef]
69. Wu, C.; Wang, L.; Harbottle, D.; Masliyah, J.; Xu, Z. Studying Bubble-Particle Interactions by Zeta Potential Distribution Analysis. *J. Colloid Interface Sci.* **2015**, *449*, 399–408. [CrossRef] [PubMed]
70. Wu, J.; Zhang, K.; Cen, C.; Wu, X.; Mao, R.; Zheng, Y. Role of Bulk Nanobubbles in Removing Organic Pollutants in Wastewater Treatment. *AMB Express* **2021**, *11*, 96. [CrossRef]
71. Frungieri, G.; Babler, M.U.; Vanni, M. Shear-Induced Heteroaggregation of Oppositely Charged Colloidal Particles. *Langmuir* **2020**, *36*, 10739–10749. [CrossRef]
72. Patterson, G.K.; Paul, E.L.; Kresta, S.M.; Etchells III, A.W. Mixing and Chemical Reactions. In *Handbook of Industrial Mixing*; John Wiley & Sons, Ltd.: Hoboken, NJ, USA, 2003; pp. 755–867; ISBN 9780471451457.
73. Cagnetta, C.; Saerens, B.; Meerburg, F.A.; Decru, S.O.; Broeders, E.; Menkveld, W.; Vandekerckhove, T.G.L.; De Vrieze, J.; Vlaeminck, S.E.; Verliefde, A.R.D.; et al. High-Rate Activated Sludge Systems Combined with Dissolved Air Flotation Enable Effective Organics Removal and Recovery. *Bioresour. Technol.* **2019**, *291*, 121833. [CrossRef]
74. Schmideder, S.; Thurin, L.; Kaur, G.; Briesen, H. Inline Imaging Reveals Evolution of the Size Distribution and the Concentration of Microbubbles in Dissolved Air Flotation. *Water Res.* **2022**, *224*, 119027. [CrossRef]
75. Arrobas, M.; Ferreira, I.Q.; Freitas, S.; Verdial, J.; Rodrigues, M.Â. Scientia Horticulturae Guidelines for Fertilizer Use in Vineyards Based on Nutrient Content of Grapevine Parts. *Sci. Hortic.* **2014**, *172*, 191–198. [CrossRef]
76. Conradie, K.; Raath, P.; Saayman, D.; Diedericks, B.; Louw, K. *Fertilisation Guidelines for The Table Grape Industry*; South African Table Grape Industry (SATI): Cape Town, South Africa, 2020; ISBN 9780620894890.